Microelectronics Reliability 51 (2011) 1985–1989

Contents lists available at ScienceDirect

Microelectronics Reliability

journal homepage: www.elsevier.com/locate/microrel

Power cycling fatigue and lifetime prediction of power electronic devices in space applications

F. Vacher *, B. Calvet, F. Mialhe

CNES, French Space Agency, 18 Avenue Edouard Belin, 31500 Toulouse, France

ARTICLE INFO

Article history:
Received 27 May 2011
Accepted 17 June 2011
Available online 13 July 2011

ABSTRACT

This paper presents a complete study about power cycling stress on space components. Power cycling fatigue is generally studied for traction or automotive applications. But power cycling failures are also a major cause of concern in space industry. In this paper we successively address the following subjects: definition of the power cycling stress in space applications, experimental power cycling test on space components and lifetime prediction for a typical earth observation application.

© 2011 Elsevier Ltd. All rights reserved.

1. Power cycling stress in space applications

1.1. Context

During a whole space mission, satellite devices can be turned ON and OFF several hundred thousand times. A very high reliability is required in space applications because of the cost of a space system and because a satellite is a non repairable system. That is why power cycling is taken into account in space applications.

A lot of studies on power cycling failures have been released for traction [1–3] and automotive [4] applications. But traction and automotive systems have totally different constraints than space systems. Current considered in traction and automotive systems are 10 or 100 times higher than in space systems. IGBT and power modules are mostly considered in transport studies, whereas small transistors are used in satellites. This paper presents a complete study about power cycling stress on space components.

Power cycling is a wear-out mechanism. There are other long term reliability concerns in space applications (radiation aging for example). Although we do not consider other constraints in this paper, it is obvious that power cycling constraint is added to other constraints during a real space mission: the combination of different wear-out mechanisms may lead to a failure.

1.2. Duration and number of cycles

There are many reasons for switching an electronic part of a satellite. For example, some equipments of a reconnaissance satellite are turned ON at each shot. Some antennas are only turned ON during the time in view of a ground station. The period of such power cycles is comprised between a few seconds and several minutes.

The average mission duration of a satellite is between 5 and 10 years. The number of power cycles can reach several hundred thousand cycles.

1.3. Space devices sensitive to power cycling stress

A wide range of component types are submitted to power cycles in a satellite: passive parts, discrete parts, microcircuits, hybrids, etc. But it is generally admitted that only power devices are subject to power cycling failures. In this paper, transistors of various powers are tested in order to determine those which are sensitive to power cycling.

2. Experimental power cycling tests

2.1. Experimental set-up

A power cycling test bench has been built for this experiment. The current and the voltage of each Device Under Test (D.U.T.) are measured and recorded during the whole experiment. The case temperature of each D.U.T. is also measured and recorded with a temperature sensor stuck on each case. Fig. 1 shows a transistor with its temperature sensor. The waveforms of the current and the temperature are shown in Fig. 2 for the test no. 10.

2.2. Conditions of each test

Only space small signal and power transistors are studied in this paper. Six different transistors have been selected and are presented in Table 1. These components have been selected to be representative of the range of transistors used in a satellite. Transistors of various powers are indeed tested (from 1 W to 150 W). Each transistor tested has been provided in a high reliability grade in order to avoid non significant results due to a bad manufacturing process. It means

* Corresponding author. Tel.: +33 5 61 28 31 12; fax: +33 5 61 28 13 30.
E-mail address: francois.vacher@cnes.fr (F. Vacher).

0026-2714/$ - see front matter © 2011 Elsevier Ltd. All rights reserved.
doi:10.1016/j.microrel.2011.06.013

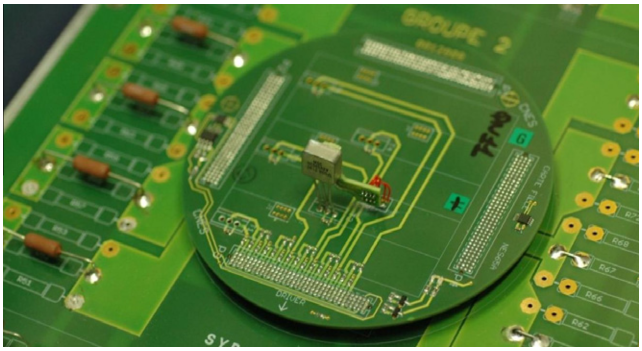

Fig. 1. D.U.T. with its temperature sensor.

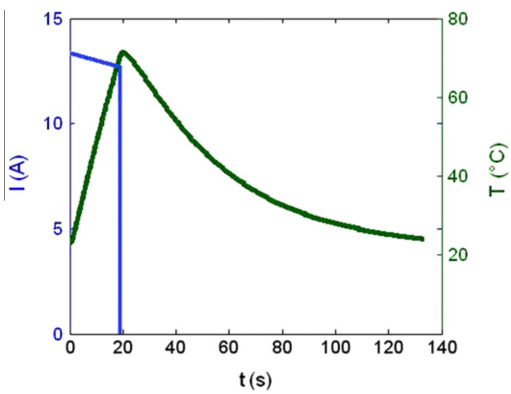

Fig. 2. Current and case temperature waveforms of a transistor 2N7224 during one cycle (test no. 10).

Table 1
Components under test.

Type	I_{MAX} (A)	P_{MAX} (W) T_C = 25 °C	Bond diameter (μm)	Reference
Bipolar	0.8	1	30	2N2222
Bipolar	2	10	180	2N5153
Bipolar	8	40	180	BUX77A
MOSFET	5.5	25	210	2N6798
Bipolar	12	~100*	250	NES65A
MOSFET	34	150	500	2N7224

* Estimated from thermal resistance data.

that each transistor has been tested according to the MIL-PRF-19500 JANTX level requirements [5] prior to be provided.

The main explanation of power cycling failures resides in the mismatch between the thermal expansion coefficient of aluminium and silicon. That is why each selected part has a die of silicon and bonding wires of aluminium.

Twelve different tests are presented in this paper. Five components are cycled in each test. The conditions of each test are detailed in Table 2. During the ON phase, the D.U.T is submitted to a constant current I and dissipates the power P. The rise of the temperature at junction level is called ΔT. The references BUX77, 2N6798 and 2N7224 are tested several times to study the influence of current and temperature on the same reference.

2.3. Results – description of the failure mechanism

Twenty-seven transistors fail during the whole experiment. Open circuit is the only failure mode. Internal inspections on each failed transistor show that bond wire lift-off is the only failure mechanism.

Table 2
Parameters of each test.

No.	D.U.T.	I (A)	I/I_{MAX} (%)	P (W)	ΔT (K)
1	2N2222	0.1	12	0.5	60
2	2N5153	1.5	75	1.2	60
3	NES65A	3	25	6	60
4	BUX77A	1.8	23	4.7	45
5	BUX77A	1.8	23	6.1	60
6	2N6798	3	54	4.2	45
7	2N6798	3	54	5.4	60
8	2N7224	13	38	12	30
9	2N7224	13	38	12	45
10	2N7224	13	38	12	60
11	2N7224	5	15	12	60
12	2N7224	13	38	12	85

Cracks propagate at the interface between the silicon chip and the aluminium wire. SEM images of lifted wire bond suggest that bond breakage occurs mainly in the chip side. As it is shown in Fig. 3, chip material remains indeed attached to the bond after lift off. This failure mechanism has been described in several papers [1,3,6] about power cycling failures. It resides in the mismatch between the thermal expansion coefficient of aluminium and silicon.

As it is shown in Fig. 4, another effect observed during this experimental campaign is reconstruction. Reconstruction is the extrusion of aluminium grains of the chip metallization.

2.4. Results

Tables 3 and 4 show the results of this experiment. In each test, 5 components are tested in the same conditions.

No failure occurred in the tests no. 1–4, 6 and 8. The numbers of cycles reached by these tests are written in Table 3.

Each part of the tests no. 9–12 has failed. N is the mean number of cycles at which a failure occurred (Table 4). Only four parts among five have failed in the tests no. 5 and 7 and these tests are still ongoing. In the test no. 11, only four components are presented instead of five because an experimental problem occurred on the 5th part.

These results confirm that power transistors are more sensitive to power cycling than small ones. A factor which partially explains this fact is that bonding wires of power transistors are bigger than small ones.

Fig. 3. SEM image of a lifted wire. Bond wire side.

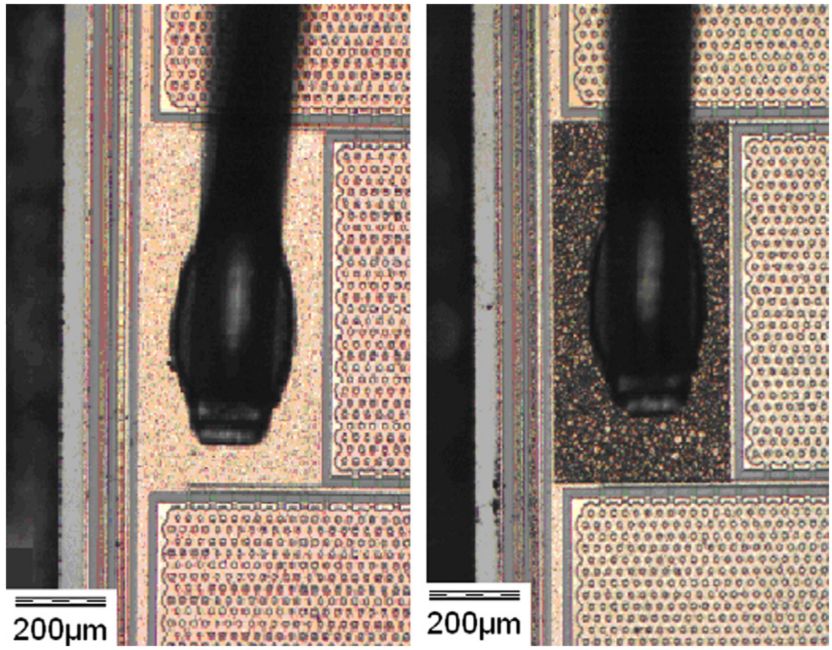

Fig. 4. Optical images of bond PAD before and after power cycling (test no. 10) – aluminium reconstruction.

Table 3
Results – Tests without failure.

Test no.	Parts failed	Number of cycles reached without failure (k)	D.U.T.	ΔT (K)
1	0/5	>500	2N2222	60
2	0/5	>300	2N5153	60
3	0/5	>300	NES65A	60
4	0/5	>300	BUX77A	45
6	0/5	>500	2N6798	45
8	0/5	>350	2N7224	30

Table 4
Results – Tests with failures.

Test no.	Parts failed	Mean number of cycles at failure (k)	D.U.T.	ΔT (K)
5	4/5	~200	BUX77A	60
7	4/5	~300	2N6798	60
9	5/5	265	2N7224	45
10	5/5	75	2N7224	60
11	4/4	108	2N7224	60
12	5/5	25	2N7224	85

2.5. Results – effect of the parameter ΔT

The tests [no. 4, no. 5], [no. 6, no. 7] and [no. 8, no. 9, no. 10, no. 12] show that N varies with ΔT. The higher is ΔT, the smaller is N. A descriptive model based on the Coffin–Manson law is widely used to model this phenomenon [1,2,4,6]. Eq. (1) gives this model, with two constant coefficients A and q:

$$N = A\Delta T^{-q} \tag{1}$$

q and A have been calculated from the results of the tests no. 9, 10 and 12. These tests are relevant to calculate these coefficients. The same reference is indeed used in these three tests with the same current. The parameter ΔT is the only parameter which differs between these three tests. Experimental data and model fitting are plotted in Fig. 5. $q = 3.9$ and $A = 6.1 \times 10^{11}$ are the best values to fit the experimental data.

The parameter A depends of each reference. This parameter is even probably different for each assembly lot of the same reference. The parameter A indeed depends of materials and processes used. The parameter $q = 3.9$ is in the same range of values than those reported in several papers about IGBT or power modules [1,2].

These results show that the failure mechanisms and models considered for power modules and IGBT in automotive and traction applications may be partially applicable to space transistors.

2.6. Results – effect of the current I

The tests no. 10 and no. 11 are relevant to understand the influence of current. They have indeed been made on the same component with the same ΔT but with different currents. The mean number of cycles at failure N and the standard deviation σ are presented for these two tests in Table 5. The standard deviation σ is calculated with the following formula:

$$\sigma = \sqrt{\frac{1}{c}\sum_{i=1}^{c}(N - N_i)^2} \tag{2}$$

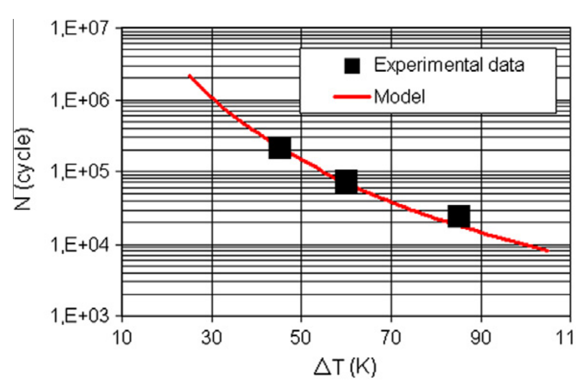

Fig. 5. Effect of the parameter ΔT. Coffin Manson model.

where c is the number of components tested (4 or 5); N is mean number of cycles at failure; N_i is the number of cycles at failure of the component i.

The standard deviation σ shows that the numbers of cycles at failure are more scattered when the current is lower. This fact is illustrated in the plot of the Weibull cumulative distribution function (Fig. 6). A physical explanation of this effect may be the following one: the bonding lift-off is mainly a fatigue mechanism and is mainly independent of the current. When the bonding wire begins to break, the resistance and the temperature of the bond probably increase. This temperature increase is more amplified with a higher current. That is why failures may occur slightly sooner and may be less scattered with a higher current. This physical explanation is partially confirmed by the failure mechanism: some parts exhibit short circuit failure only at high temperature and remain functional at room temperature. Internal visual inspections on these parts show that bonding wires were still in contact with the die at room temperature. Bond pull tests confirm that the bonding wires were not attached anymore with the die.

3. Life time prediction for space applications

3.1. Typical mission profile

A typical mission profile is used in this paper to make a lifetime prediction. This example corresponds to a transistor used in a measurement equipment mounted on a satellite in low earth orbit (LEO). The lifetime of the mission is 8 years and the total number of ON/OFF cycles is 150,000. The junction temperature rise is the sum of two main terms: the temperature rise at equipment level varying with a period of one orbit and the temperature rise at board and component levels occurring at each use of the equipment.

Rainflow-counting method is used to extract the number and the amplitude of the thermal cycles which are experienced by the device. This method is widely used in mechanical evaluation of cumulated fatigue. It can be easily computed with the algorithm described in the standard [7]. The thermal cycles histogram counted according to this method is presented in Fig. 7.

3.2. Lifetime prediction

The Miner's law [8] is widely used to add cycles at different temperature excursions under the hypothesis of linear accumulation of the cyclic fatigue damage. Consider a component which has been submitted to cycles at different various excursions. The Miner's law states that failure occurs when:

$$1 = \sum_k \frac{n_k(\Delta T_k)}{N_k(\Delta T_k} \tag{3}$$

where n_k is the number of cycles performed at a given thermal excursion ΔT_k and N_k the number of cycles at failure at the same ΔT_k.

The number n (ΔT) of cycles at ΔT equivalent to the sum of cycles at different ΔT_k can be derived from Coffin–Manson's law (1) and Miner's law (3):

$$n(\Delta T) = \Delta T^{-q} \sum_k \frac{n_k}{\Delta T_k^{-q}} \tag{4}$$

Table 5
Results – Effect of the current.

No.	D.U.T.	ΔT (K)	I (A)	N (k)	σ (k)
10	2N7224	60	13	75	11
11	2N7224	60	5	108	30

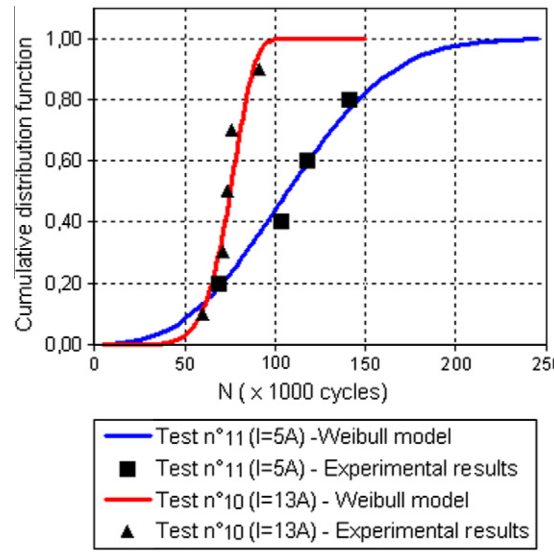

Fig. 6. Effect of the current. Plot of the Weibull cumulative distribution function for the tests nos. 10 and 11.

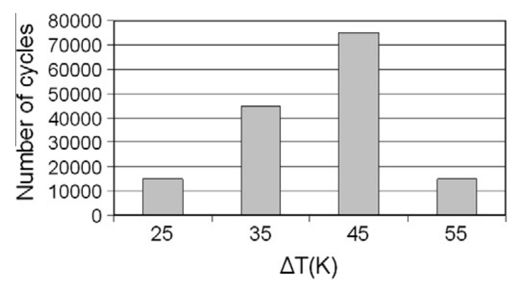

Fig. 7. Thermal cycles histogram considered in the lifetime prediction.

The number of cycles at $\Delta T = 60$ K corresponding to the whole mission calculated with Eq. (4) is about 40,000 cycles. This number is in the same range of values than the maximum number of cycles at $\Delta T = 60$ K of the reference 2N7224 (test no. 10, $N - 3\sigma = 42{,}000$ cycles). Such an example shows why power cycling is a cause of concern in space industry. This example shows also that only the most powerful transistors (2N7224 in this example) of missions with a high number of cycles (150,000 cycles in this example) are concerned by this failure mode.

4. Conclusion

This paper presents a complete study about power cycling stress in space applications. Satellite's devices are sometimes cycled several hundred thousand times.

A power cycling experiment made on space devices is described. This experiment shows that space components may exhibit failures at less than 10^5 cycles with $\Delta T = 60$ K. The failure mechanism and the influence of various parameters on the maximum number of cycles are studied. This experiment shows that the failure mechanisms and models considered for power modules and IGBT in automotive and traction applications may be partially applicable to space transistors. This result is very useful for risk analysis of space projects.

Based on a realistic mission profile, a lifetime prediction is made. It shows that the power cycling constraint of a space mission may be in the same range than the power cycling robustness of a space power transistor. It justifies the use of appropriate margins in space electronic board design.

References

[1] Mermet-Guyennet M, Perpina X, Piton M. Revisiting power cycling test for better life-time prediction in traction. In: Proceedings of European symposium on reliability of electron devices, failure physics and analysis (ESREF); 2007.
[2] Ciappa M, Fichtner W. Lifetime Prediction of IGBT Modules for Traction Applications. IEEE Int Reliability Physics Symp 2000;38:210–6.
[3] Onuki J, Koizumi M, Suwa M. Reliability of thick Al wire bonds in IGBT modules for traction motor drives. IEEE Trans Adv Packag 2000;23(1):108–12.
[4] Ciappa M, Carbognani F, Fichtner W. Lifetime prediction and design of reliability tests for high-power devices in automotive applications. IEEE Trans Dev Mater Reliab 2003;3(4):191–6.
[5] MIL-PRF-19500. General specification for semiconductor devices. Revision P. 20/10/2010. Military specification of Defense Supply Center Columbus.
[6] Ciappa M. Selected failure mechanisms of modern power modules. Microelectron Reliab 2002;42:653–67.
[7] ASTM E-1049. Standard practices for cycle counting in fatigue analysis; 1985.
[8] Miner MA. Cumulative damage in fatigue. J Appl Mech 1945;12:159–64.